

DISCOVERY OF TWO VERY WIDE BINARIES WITH ULTRACOOOL COMPANIONS AND A NEW BROWN DWARF AT THE L/T TRANSITION

KORALJKA MUŽIĆ^{1,*}, JACQUELINE RADIGAN¹, RAY JAYAWARDHANA¹, VALENTIN D. IVANOV², JACQUELINE K. FAHERTY^{3,6},
RADOSTIN G. KURTEV⁴, ALEJANDRO NÚÑEZ^{5,6}, HENRI M. J. BOFFIN², OLIVIER HAINAUT⁷, KELLE CRUZ^{5,6}, DAVID JONES²,
STANIMIR METCHEV⁸, AMY TYNDALL², JURA BORISSOVA^{4,9}

Draft version May 25, 2022

ABSTRACT

We present the discovery and spectroscopic follow-up of a nearby late-type L dwarf (2M0614+3950), and two extremely wide very-low-mass binary systems (2M0525-7425AB and 2M1348-1344AB), resulting from our search for common proper motion pairs containing ultracool components in the Two Micron All Sky Survey (2MASS) and the Wide-field Infrared Survey Explorer (WISE) catalogs. The near-infrared spectrum of 2M0614+3950 indicates a spectral type $L9 \pm 1$ object residing at a distance of 26.0 ± 1.8 pc. The optical spectrum of 2M0525-7425A reveals an $M3.0 \pm 0.5$ dwarf primary, accompanied by a secondary previously classified as L2. The system has an angular separation of $\sim 44''$, equivalent to ~ 2000 AU at distance of 46.0 ± 3.0 pc. Using optical and infrared spectra, respectively, we classify the components of 2M1348-1344AB as $M4.5 \pm 0.5$ and $T5.5 \pm 1$. The angular separation of $\sim 68''$ is equivalent to ~ 1400 AU at a distance of 20.7 ± 1.4 pc. 2M1348-1344AB is one of only six very wide (separation > 1000 AU) systems containing late T dwarfs known to date.

Subject headings: binaries:general - stars:low-mass, brown dwarf - stars: individual
(2MASSJ06143818+3950357, 2M05254550-7425263, 2M05253876-7426008,
2M13480721-1344321, 2M13480290-1344071)

1. INTRODUCTION

The formation and evolution of objects at the low-mass end of the initial mass function is one of the most fundamental and yet not fully understood issues in our current picture of how stars form and evolve. The existence of brown dwarfs (BDs; $m < 0.08 M_{\odot}$) down to $\sim 7 M_J$ can be explained within the standard framework of star formation (Low & Lynden-Bell 1976). By including additional physics such as turbulence (Padoan & Nordlund 2004), dynamical interactions (Boffin et al. 1998; Bate 2009), disk fragmentation (Stamatellos & Whitworth 2009), and/or photo-erosion from nearby bright stars (Whitworth & Zinnecker 2004), one can create objects with even lower masses (down to $3 M_J$). The relative importance of these mechanisms in producing the Galactic substellar population is unclear. The key here is to confront predictions from the various scenarios with

observational results. One means of testing these theories is through the empirical characterization of very-low-mass (VLM) multiple systems. As summarized in Burgasser (2007), these systems are observed to be less frequent, more tightly bound, and of higher mass ratios than their more massive counterparts.

Wide binaries are of interest because their large separations (greater than 100 AU) and low binding energies provide direct constraints for formation models. For example, wide binaries are expected to be disrupted during the ejection process. This directly challenges the ejection model for the formation of VLM stars and BDs (Reipurth & Clarke 2001; Bate & Bonnell 2005). Several other models have been successful in creating wide VLM binaries, e.g. by fragmentation during the cluster formation (Bate 2009), in fragmenting disks (Stamatellos & Whitworth 2009), or by dynamical capture during star cluster dissolution phase (Kouwenhoven et al. 2010; Moeckel & Clarke 2011). The models by Bate (2009) and Kouwenhoven et al. (2010) predict the frequency of binaries with separations > 1000 AU to be a few percent, compared with a fraction of $\sim 10\%$ found observationally for nearby (Lépine & Bongiorno 2007; Longhitano & Binggeli 2010) and young (Kraus & Hillenbrand 2009) stars. In star forming regions, the fraction of wide binaries appears to decrease with decreasing stellar mass (Kraus & Hillenbrand 2009). While the number of known wide binaries containing ultracool components is constantly growing as more searches are performed, they are mostly reported in an individual fashion, rather than in complete samples that would allow us to assess their true frequency.

Despite the effort that has been devoted to modeling over the past decade, evolutionary tracks and atmosphere models for ultracool objects still suffer from uncertain-

kmuzic@eso.org

¹ Department of Astronomy & Astrophysics, University of Toronto, 50 St. George Street, Toronto, ON M5S 3H4, Canada

² European Southern Observatory, Alonso de Córdova 3107, Casilla 19, Santiago, 19001, Chile

³ Department of Astronomy, University of Chile, Camino El Observatorio 1515, Casilla 36-D, Santiago, Chile

⁴ Departamento de Física y Astronomía, Facultad de Ciencias, Universidad de Valparaíso, Av. Gran Bretaña 1111, Playa Ancha, Casilla 53, Valparaíso, Chile

⁵ Department of Physics and Astronomy, Hunter College, City University of New York, 695 Park Ave, NY 10065, USA

⁶ Dept. of Astrophysics, American Museum of Natural History, New York, NY, 10024, USA

⁷ European Southern Observatory, Karl-Schwarzschild-Strasse 2, D-85748 Garching bei München, Germany

⁸ Department of Physics and Astronomy, Stony Brook University, 100 Nicolls Rd, Stony Brook, NY 11794-3800

⁹ The Milky Way Millennium Nucleus, Av. Vicuña Mackenna 4860, 782-0436 Macul, Santiago, Chile

* Present address: ESO Chile ²

ties. Widely separated L and T dwarf companions to nearby stars are also valuable for studying the evolution and atmospheres of brown dwarfs. The possibility for independent determination of age, mass, and metallicity makes these brown dwarfs benchmark objects for calibration of evolutionary models and atmospheric studies (Pinfield et al. 2006; Burgasser et al. 2010a; Loutrel et al. 2011).

The transition between the spectral types L and T occurs over a small temperature range of 200-300 K (Kirkpatrick et al. 2000; Dahn et al. 2002; Tinney et al. 2003), and is believed to be caused by the depletion of condensate clouds, where the driving mechanism for the depletion is inadequately explained by current cloud models (Ackerman & Marley 2001; Burgasser et al. 2002; Knapp et al. 2004). The complex dynamic behavior of condensate clouds of low temperature atmospheres at the L/T transition is one of the leading problems in brown dwarf astrophysics today (Tinney & Tolley 1999; Bailer-Jones & Mundt 1999; Goldman 2005; Artigau et al. 2009; Radigan et al. 2012).

In this paper we report the discovery of a brown dwarf at the L/T transition, and two nearby wide binaries consisting of M-dwarf primaries with early L-type and late T-type companions¹¹.

2. SEARCH FOR WIDE BINARIES CONTAINING ULTRACOOL DWARFS

We performed a cross-match between the Two Micron All Sky Survey (2MASS) catalog and the Wide-field Infrared Survey Explorer (WISE) Preliminary Data Release catalog, in order to search for common proper motion pairs containing at least one very-low-mass component. Following the successful approach of Radigan et al. (2008, 2009), the correlation of catalogs, calculation of proper motions, and identification of co-moving stars was done in overlapping sections of 4 deg^2 of the sky at a time. For every WISE source, we found the closest 2MASS match and computed proper motion vectors with uncertainties. We then selected stars that had moved at $> 3\sigma$ level compared to all others within the search area. Stars within $120''$ of one another with proper motion amplitudes agreeing within 2σ and proper motion components agreeing within 1σ in either right ascension or declination were flagged as potential binaries. Towards the end of writing this paper, the new all-sky release of the WISE catalog became available. We have repeated the proper motion measurements for the 4 deg^2 fields around the three objects reported here. The main reason for repeating these measurements is the improved astrometry for the faint sources in the new catalog. The uncertainties in declination in the WISE preliminary catalog were computed by adding $0.5''$ in quadrature to the extraction measurement uncertainty to reflect the impact of the declination bias error known to affect a large fraction of sources fainter than $W1 \sim 13 \text{ mag}$. This has been corrected in the new release. Thus, while the main search for binaries has been performed using the preliminary version, listed proper motions and photometry are based on the all-sky release of the WISE catalog.

Kirkpatrick et al. (2011) recently published a compilation of 2MASS and WISE photometry for ~ 350 early M- to late T-dwarfs. Mid-infrared WISE photometry is particularly suitable for L/T dwarf selection, because of their red $W1 - W2$ colors, which are almost unique among astrophysical sources. Additionally, $W2 - W3$ color can be used to distinguish between BDs on the one side, and AGB stars and dust-obscured galaxies on the other (Eisenhardt et al. 2010). In the following, we describe the procedure for selection of the candidate binary systems suitable for spectroscopic follow-up. First, we required A, B or C photometric quality flags for J , H , K , $W1$, $W2$ and $W3$ photometry for all the components of the potential binary systems. After this initial flagging, we were left with ~ 11000 objects. We then rejected all candidates for which at least one of the components does not satisfy the following conditions: located to the left of the solid line in the $W2 - W3$ vs. $W1 - W2$ diagram (Figure 1 left), $J - H$ between -1 and 2 , $W2 - W3 > -0.5$, $J - W2 > 0.5$, and $W1 - W2 > 0.35$. The latter condition was applied to discard a large group of contaminants that occupy the color space with $W1 - W2 \lesssim 0.3$ and $J - W2 < 6$ in the right panel of Figure 1. Relaxing this condition to $W1 - W2 > 0$ results in ~ 1200 candidates. By applying the cut at $W1 - W2 = 0.35$, we were left with only 19 candidates. Clearly, this restriction makes our search insensitive to essentially all M-M pairs, and a large portion of L-type companions earlier than L6 will be discarded as well. After applying the color cuts on either of the components of a candidate binary system, we inspected the remaining 19 candidates visually, in order to remove false positives. In most cases these contain blends of unresolved source pairs in WISE, due to significantly lower resolution when compared with 2MASS.

Two color-color diagrams used for the selection are shown in Figure 1. Color-coded dots show the colors of M, L and T dwarfs taken from Kirkpatrick et al. (2011), while the black symbols show the objects reported in this paper. In the following subsections we describe the three discoveries reported in this paper, along with the known parameters obtained from the literature.

2MASS and WISE photometry for the objects reported in this paper are listed in Table 1. Table 2 contains the proper motions and other physical properties of the objects discussed in the next sections.

2.1. 2M0614+3950

2M06143818+3950357 (hereafter 2M0614+3950) was at first identified as a companion to 2M06143791+3951202. With $W2 - W3 \approx 3$, $W1 - W2 \approx 0$, and $J - W2 \approx 0.75$, the latter object is marginally consistent with being an early M-dwarf. However, an M0 dwarf as faint as $J = 16.3$ would have to be at a distance larger than 1kpc. By checking the optical catalogs of the region, we found that the optical source matching 2M06143791+3951202 has essentially the same position as the 2MASS source (offset of $\sim 0.2''$ from GSC2.2 and USNO-B1 catalog positions), whereas at the measured proper motion we would expect an offset of $\sim 2.5''$ between the GSC2.2 and 2MASS, and $> 5''$ between USNO-B1 and 2MASS. Furthermore, in the optical images the position reported by WISE appears to be located between the source matching the 2MASS position and another faint (R ~ 19)

¹¹ One of the two binaries, 2M1348-1344, was independently discovered by Deacon et al. (2012)

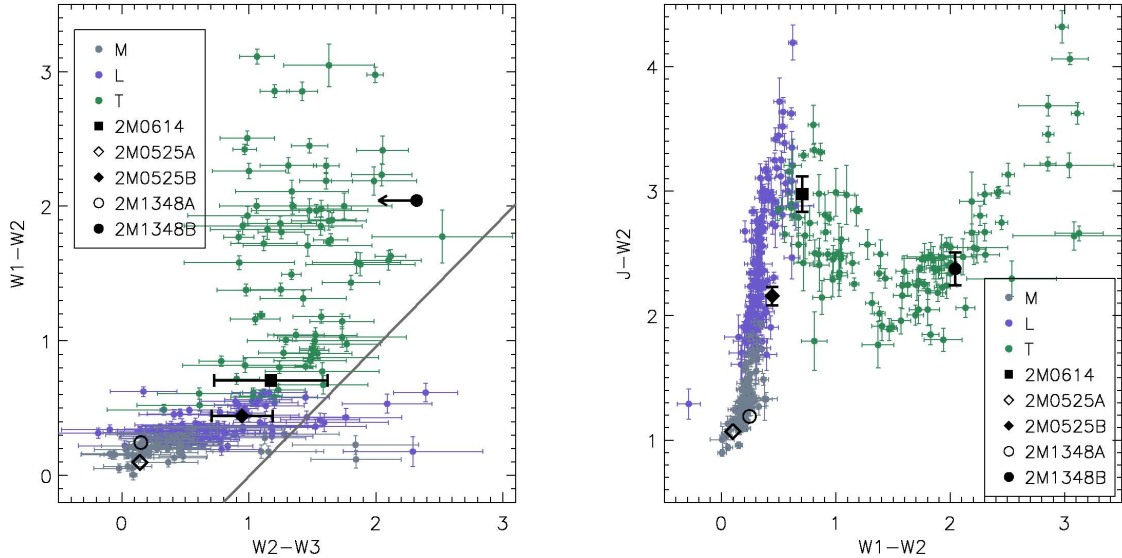


FIG. 1.— 2MASS and WISE color-color diagrams used for color selection of the MLT dwarf candidates. Diamonds and circles show the components of the two new wide binaries 2M0525-7425 and 2M1348-1344, respectively, while the filled square shows the new L9 dwarf 2M0614+3950. Dots show the colors of the known MLT dwarfs from Kirkpatrick et al. (2011). The solid line in the left panel is used to eliminate extragalactic sources to the right of the line from the bulk of the M, L, and T dwarfs to the left (Kirkpatrick et al. 2011). We do not plot error-bars in cases where they are comparable to or smaller than the plotting symbol.

source not detected by 2MASS. We thus conclude that the WISE source identified here as a potential primary of a binary system is most probably a blend. The suspected secondary, however, has colors that are consistent with a late-L or an early-T ultracool dwarf, and was therefore included in our spectroscopic follow-up.

2.2. 2M0525-7425

A common proper motion pair here denoted as 2M0525-7425 consists of the primary 2M05254550-7425263 and the secondary 2M05253876-7426008. Both objects were reported by Kirkpatrick et al. (2010) as part of a large-area proper motion survey. The secondary was observed with GMOS/Gemini during their spectroscopic follow-up, and was assigned the optical spectral type L2. The primary was also reported by Subasavage et al. (2005) as a high-proper motion source at a photometric distance of 28.7 pc. Despite the matching proper motions, the pair was never reported as a wide binary candidate; the primary lacked spectral classification.

2.3. 2M1348-1344

A common proper motion pair here denoted as 2M1348-1344 consists of the primary 2M13480721-1344321 (also known as LP 738-14, NLTT 35266, LHS 2803) and the secondary 2M13480290-1344071. Reid et al. (2003) published photometry of the primary, from which they estimate distance of 20.9 pc. Casagrande et al. (2008), again based on photometry, estimated an effective temperature of $T_{\text{eff}} = 2942 \pm 58$ K. The secondary has colors consistent with late T-dwarfs (Figure 1).

3. SPECTROSCOPIC FOLLOW-UP

3.1. EFOSC2/NTT

We obtained optical spectroscopy of 2M0525-7425A (December 23 2011; program ID 184.C-1143(E)) and 2M1348-1344A (February 29 2012; 088.D-0573(A))

with the ESO Faint Object Spectrograph and Camera (EFOSC2; Buzzoni et al. 1984) on the ESO New Technology Telescope (NTT). Observations were taken in long-slit mode with a $1''$ slit and grism #05, covering wavelengths 5200Å-9350Å with a resolution of 16.6Å. The data were flat-fielded, extracted, wavelength- and flux-calibrated using the EFOSC2 pipeline provided by ESO. The EFOSC2 grism #05 used in this work introduces strong fringing redwards of about ~ 7200 Å. In the case of 2M1348-1344A the afternoon dome flats adequately removed the fringing, while the effect remains present in the spectrum of 2M0525-7425A. The imperfect flat-fielding is due to telescope/instrument flexure, which may cause a slight positional mismatch between the fringes in the dome flats and science images. The signal-to-noise ratio, as measured by the iraf task *splot* varies between 5 and 18 for 2M0525-7425A, and 5 and 23 for 2M1348-1344A.

3.2. SpeX/IRTF

We obtained near-infrared spectroscopy of 2M0614+3950 on December 8 2011 with SpeX (Rayner et al. 2003) on the NASA Infrared Telescope Facility (IRTF) on Mauna Kea. We used the low-resolution prism mode of SpeX to provide a wavelength coverage of 0.8-2.5 microns in a single order and an average resolution of $R \sim 120$ with a $0''.5$ -wide slit. The spectrum was acquired using the 0.5-wide slit aligned at parallactic angle, with an airmass that ranged from 1.08 to 1.17 during the observations. The target was observed with multiple exposures, dithering in an ABBA pattern along the slit, with a total integration time of 2880 sec. After the target observation, a nearby A0 star at a similar airmass to the target was observed for both telluric and flux calibration. Internal flat field and argon arc lamp calibration frames were obtained at the target position for pixel response and wavelength calibration.

TABLE 1
 2MASS AND WISE PHOTOMETRY

name	α^a	δ	J	H	K	W1	W2	W3	W4
2M1348-1344A	13 48 07.22	-13 44 32.1	10.41 ± 0.02	9.94 ± 0.02	9.66 ± 0.02	9.46 ± 0.02	9.24 ± 0.02	9.11 ± 0.03	8.72 ± 0.33
2M1348-1344B	13 48 02.91	-13 44 07.2	16.48 ± 0.12	16.09 ± 0.17	> 16.45	16.15 ± 0.07	14.18 ± 0.05	> 12.14	> 9.14
2M0525-7425A	05 25 45.50	-74 25 26.3	10.03 ± 0.02	9.42 ± 0.02	9.21 ± 0.02	9.08 ± 0.02	8.97 ± 0.02	8.82 ± 0.02	8.53 ± 0.15
2M0525-7425B	05 25 38.76	-74 26 00.8	15.71 ± 0.07	14.97 ± 0.10	14.43 ± 0.10	14.02 ± 0.03	13.57 ± 0.03	11.97 ± 0.12	> 9.46
2M0614+3950	06 14 38.18	+39 50 35.7	16.59 ± 0.14	15.60 ± 0.12	15.02 ± 0.12	14.33 ± 0.03	13.66 ± 0.04	12.19 ± 0.34	> 9.22

^a coordinates from 2MASS

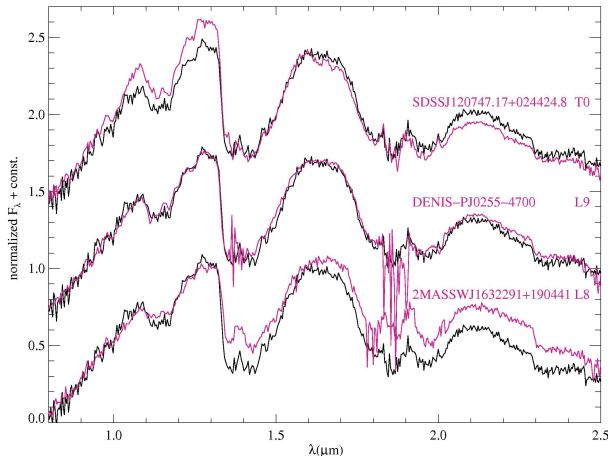


FIG. 2.— SpeX spectrum of 2M0614+3950 shown in black, with the standard spectral sequence of ultracool dwarfs at the L/T transition (Burgasser et al. 2006a; Burgasser 2007;Looper et al. 2007). All spectra were normalized at $1.6\mu\text{m}$.

The spectral data was extracted, flat-fielded, wavelength calibrated, telluric corrected, and flux-calibrated with the *SpeXtool* reduction package (Cushing et al. 2004; Vacca et al. 2003). The signal-to-noise ratio of the final spectrum varies between 6 and 36.

3.3. FIRE/Magellan

We obtained near-infrared spectroscopy of 2M1348-1344B on March 20 2012 with the Folded-port InfraRed Echelette (FIRE; Simcoe et al. 2008, 2010) spectrograph on the 6.5-m Magellan Baade Telescope. In its high throughput prism mode, FIRE covers the wavelength range from 0.8 to $2.5\mu\text{m}$ at a resolution ranging from $R=500$ at J -band to $R=300$ at K -band for a slit width of $0.6''$. A series of ABBA nod pairs taken with exposure times of 120s per position were used giving a total exposure time of 480s. The spectrograph detector was read-out using the 4-amplifier mode at high gain (1.2 counts per e^-) with the SUTR sampling mode. We also obtained exposures of a variable voltage quartz lamp for flat-fielding purposes and neon/argon arc lamps were used for wavelength calibration. The A0 dwarf star HIP70419 was used for telluric and flux calibration. Data were reduced with the new FIRE pipeline tools implemented in IDL and written by R. Simcoe, J. Bochanski and M. Matejek. The signal-to-noise ratio of the final spectrum varies between 4 and 14.

4. RESULTS AND DISCUSSION

4.1. 2M0614+3950: New brown dwarf at L/T transition

The spectrum of 2M0614+3950 is well matched by the L9 near-infrared spectral template. In Figure 2 we show

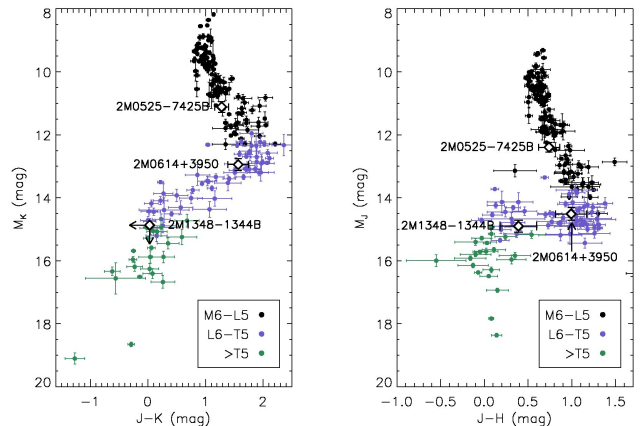


FIG. 3.— Color-magnitude diagrams showing ultracool dwarfs with parallaxes from Table 10 of Dupuy & Liu (2012) with errors ≤ 0.5 mag. Objects at the L/T transition are shown as purple circles. The absolute magnitude of 2M0614+3950 (L9) was calculated assuming a distance of $d=26.0 \pm 1.8$ pc; for 2M1348-1344B (T5.5) we use $d=20.7 \pm 1.4$ pc, and for 2M0525-7425 (L2) $d=46.0 \pm 3.0$ pc.

the comparison of the spectrum of our target (black) and the SpeX NIR standards from L8 to T0 (Burgasser et al. 2006a; Burgasser 2007;Looper et al. 2007).

Dupuy & Liu (2012) provide a comprehensive update to the absolute magnitudes of ultracool dwarfs with measured parallaxes as a function of spectral type, for a wide variety of broad-band filters including 2MASS and WISE passbands. We use the relations between absolute J , H , K , $W1$, and $W2$ magnitudes and spectral type to calculate the distance to 2M0614+3950. The distance is calculated as a weighted average of the five estimates, with the weights equal to the inverse square of the individual uncertainties. These include the rms uncertainty of the polynomial fits given in Dupuy & Liu (2012), uncertainty of one spectral subtype, and the photometric errors. For an object of spectral type L9 we obtain $d=26.0 \pm 1.8$ pc. However, based on the recent analysis of the parallaxes for 70 nearby ultracool dwarfs, Faherty et al. (2012) point out that the brightening across the L/T transition is more pronounced in reality than when represented by the polynomial fits of absolute magnitudes versus spectral type. Therefore, in addition to the polynomial fits, they calculate linear piecewise functions for three spectral type regions. The distance obtained from the polynomial fits in Faherty et al. (2012) is in agreement with the above estimate. The piecewise fits, however, locate the object somewhat closer, at ~ 22 pc (average from JHK estimates). We note that distances for objects at the L/T transition are uncertain as we are still investigating their significant scatter in luminosity.

Figure 3 shows the position of 2M0614+3950 in NIR

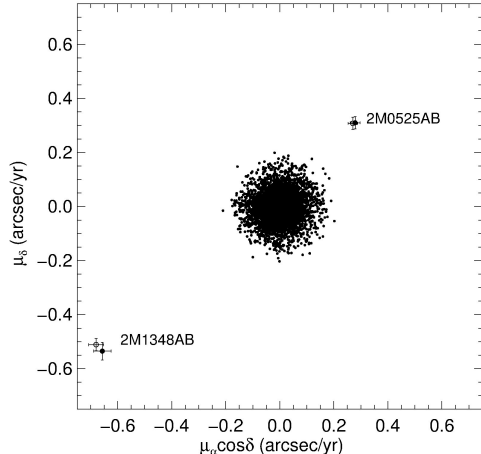


FIG. 4.— Proper motions of the sources within 1 deg^2 around 2M0525-7425 and 2M1348-1344. The components of the wide binary candidates 2M0525-7425 and 2M1348-1344 are marked with the open (primary) and filled (secondary) circles with corresponding errorbars.

color-magnitude diagrams, alongside ultracool dwarfs with parallaxes and errors $\leq 0.15 \text{ mag}$ from Dupuy & Liu (2012). 2M0614+3950 is located in the region mainly populated by ultracool dwarfs of spectral type between $\sim \text{L7}$ and $\sim \text{T2}$. Since the distance to the object was calculated assuming the absolute magnitude of an L9 dwarf, its placement in the correct magnitude range is assured. The colors of 2M0614+3950 are consistent with the L7 - T2 spectral range and do not show any peculiarities.

Using the relations between effective temperature and spectral type (Stephens et al. 2009), and absolute bolometric magnitude and spectral type (Burgasser 2007), we obtain $T_{\text{eff}} \approx 1350 \pm 110 \text{ K}$, and $\log(L/L_{\odot}) = -4.61 \pm 0.10$. The uncertainties are derived by adding in quadrature the rms error of the polynomial fits and the error resulting from the uncertainty of one spectral subtype. Compared to the DUSTY theoretical isochrones (Chabrier et al. 2000; Baraffe et al. 2002), this would correspond to an object with a mass of $\sim 0.04 - 0.07 M_{\odot}$, for the ages of 1-10 Gyr. A summary of the observational and physical properties of 2M0614+3950 is given in Table 2.

4.2. 2M0525-7425: New wide M/L binary

Figure 4 shows proper motions of the sources within 1 deg^2 around 2M0525-7425 and 2M1348-1344. The matching radius was set to $2''$ in order to discard mismatches caused by faint 2MASS sources not detected in WISE. The components of the wide binary 2M0525-7425 are marked with open (primary) and filled (secondary) circles with errorbars, which are calculated by combining the astrometric uncertainties of the sources in 2MASS and WISE catalogs.

In Figure 5 we show the comparison of the spectrum of the primary (black) and CTIO-4m and CTIO-1.5m spectra of dwarfs with spectral types from M2 to M4 (purple). The comparison spectra were taken from www.dwarfarchives.org, and were chosen to match the EFOSC2 wavelength coverage. The spectrum of 2M0525-7425A is well matched by the spectra of M2.5 - M3.5 dwarfs. We therefore assign it a spectral type $\text{M3} \pm 0.5$.

Reid & Cruz (2002) computed color-magnitude rela-

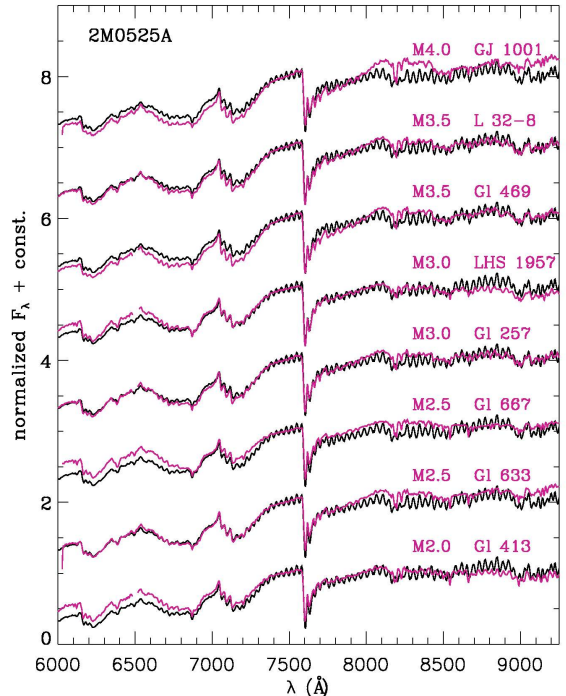


FIG. 5.— EFOSC2 spectrum of 2M0525-7425A shown in black, with the spectral sequence of early M-dwarfs from dwarfarchives.org overplotted in purple. The comparison spectra were chosen to have broad wavelength coverage similar to our data, and were smoothed to match the resolution of the object spectrum. All spectra were normalized at 7500 \AA .

tions in the $(M_V, V - K)$, $(M_V, V - I)$, and $(M_I, I - J)$ planes for nearby stars with well-determined trigonometric parallaxes, which allows us to determine a photometric parallax for 2M0525-7425A. We use JK photometry from 2MASS, $V=13.57$ (NOMAD catalog; Zacharias et al. 2005), and $I=11.3$ (DENIS catalog). Combining the results from the three relations in Reid & Cruz (2002), we obtain a distance of $d=43.9 \pm 4.3 \text{ pc}$. The distance is calculated as a weighted average of the three estimates, with the weights equal to the inverse square of the individual uncertainties resulting from the scatter of the color-magnitude relations given in Reid & Cruz (2002). The photometric uncertainties are either negligible compared to the fit errors (IJK), or not available (V), and therefore were not included in the calculation.

The distance to 2M0525-7425B can be estimated in the same way as for 2M0614+3950 (see Section 4.1). The secondary was classified as an L2 dwarf (Kirkpatrick et al. 2010): we estimate that it lies at a distance $d=48.0 \pm 4.3 \text{ pc}$. The excellent agreement between independent distance estimates for the two objects gives support to the wide-binary nature of the pair. In the following, we adopt the weighted average $d=46.0 \pm 3.0 \text{ pc}$ as the distance to the 2M0525-7425 binary, with the weights equal to the inverse square of the component distance uncertainties. At this distance, the projected separation of $43.9'' \pm 0.1''$ is equivalent to $2020 \pm 130 \text{ AU}$. The uncertainty of the projected separation combines the astrometric errors of the binary components from 2MASS.

Using the relations between effective temperature and spectral type (Stephens et al. 2009), and absolute bolo-

metric magnitude and spectral type (Burgasser 2007), we obtain $T_{\text{eff}} \approx 1970 \pm 120$ K, and $\log(L/L_{\odot}) = -3.79 \pm 0.11$ for the L2 companion. The spectral type for this source is adopted from Kirkpatrick et al. (2010), which gives no formal errors on spectral types. We therefore assume an uncertainty of 0.5 subtypes, that is equal to the step in their spectral typing scheme. The resulting uncertainty was added in quadrature to the scatter of the polynomial fits. For the primary, we use relations between effective temperature and color determined by Casagrande et al. (2008) for a large sample of nearby M dwarfs with accurate optical and infrared photometry. We calculate T_{eff} as the average of the estimates based on six optical-to-near-infrared colors (V and R versus J, H, and K), with the uncertainty equal to the standard deviation of these six estimates. The R magnitude originates from the HST Guide Star Catalog-II (GSC-II)¹². We obtain $T_{\text{eff}} \approx 3320 \pm 50$ K. From the relation between the 2MASS and bolometric magnitudes we obtain $\log(L/L_{\odot}) = -1.60 \pm 0.03$. The uncertainty takes into account the scatter of the linear relations between JHK and bolometric magnitudes (Casagrande et al. 2008), photometric errors, and the distance uncertainty.

Lépine et al. (2007) defined the metallicity dependent index ζ using the CaH2, CaH3 and TiO5 molecular band heads in the optical, recently re-calibrated by Dhital et al. (2012). From the EFOSC2 spectrum of 2M0525-7425A we find $\zeta_L = 0.94$ and $\zeta_D = 0.89$, placing the object among the dwarf metallicity class. However, while the ζ -index can be very useful for discriminating between different metallicity classes, its correlation with $[\text{Fe}/\text{H}]$ within the dwarf metallicity class ($\zeta > 0.825$) is weak and shows a significant scatter (Lépine et al. 2012). The location of M dwarfs in the $(V - K_S) - M_{K_S}$ color-magnitude diagram has been shown to correlate with metallicity (Bonfils et al. 2005; Johnson & Apps 2009; Schlaufman & Laughlin 2010). Using the relation from Schlaufman & Laughlin (2010), who improved upon previous calibrations, and adopting the average distance to the binary $d = 46.0 \pm 3.0$ pc, we obtain $[\text{Fe}/\text{H}] = -0.01 \pm 0.03$ for 2M0525-7425A. The final uncertainty combines the uncertainties of the distance and the K_S magnitude, while the error of the V magnitude is not available. Note that Neves et al. (2012) find the rms dispersion of the Schlaufman & Laughlin (2010) relation to be 0.19 ± 0.03 dex.

West et al. (2008) showed that the decrease in the fraction of magnetically active stars (as traced by $\text{H}\alpha$ emission) as a function of the vertical distance from the Galactic plane can be explained by thin-disk dynamical heating and a rapid decrease in magnetic activity. The timescale for this rapid activity decrease changes according to the spectral type. From the lack of $\text{H}\alpha$ emission in the spectrum of 2M0525-7425A, we place a lower limit for its age at 1.5 Gyr.

Assuming an age of 1-10 Gyr, the component masses can be estimated from evolutionary models. By comparing the derived absolute JHK_S magnitudes with the BCAH98 evolutionary models (Baraffe et al. 1998), we find a mass of $0.46 \pm 0.01 M_{\odot}$ for the primary. The adopted uncertainty was determined by varying the absolute magnitudes within their corresponding uncertain-

ties. This result is in agreement with the value $0.45 \pm 0.01 M_{\odot}$ obtained using the empirical mass-luminosity relationship of Delfosse et al. (2000). For the secondary, we find a mass of $0.070^{+0.005}_{-0.010} M_{\odot}$, with an error reflecting the model grid spacing. The mass ratio of 2M0525-7425AB is 0.15 ± 0.02 , which is relatively low for a low-mass pair. The mass ratios are discussed in Section 5.2. A summary of observational and physical properties of 2M0525-7425AB is given in Table 2.

4.3. 2M1348-1344: New wide M/T binary

In the left panel of Figure 6 we show the comparison of the EFOSC2 spectrum of the primary (black) and the CTIO-4m and CTIO-1.5m spectra of dwarfs with spectral types from M4 to M5 (purple). The comparison spectra were taken from www.dwarfarchives.org, and were chosen to match the EFOSC2 wavelength coverage. Based on this plot, we assign 2M1348-1344A a spectral type of $M4.5 \pm 0.5$. The FIRE spectrum of the secondary is shown in black in the right panel of Figure 6, along with the SpeX NIR standards from T4 to T8 (Burgasser et al. 2004, 2006a). Spectral templates T5 and T6 both provide good fit to the spectrum of 2M1348-1344B. As a check, we calculate the spectral indices from Burgasser et al. (2006a), that are based on the strength of the major H_2O and CH_4 bands in the near-infrared. Five indices yield spectral types from T5 to T7, with the average of T5.7. We type 2M1348-1344B as $T5.5 \pm 1.0$.

The distance to the primary can be calculated in the same way as for 2M0525-7425A (Section 4.2), adopting $V = 15.1$ and $I = 12.1$ (Reid et al. 2003). This gives us $d = 21.5 \pm 2.1$ pc. The distance to the T-dwarf was calculated in the same way as for the L2 and L9 dwarfs from the previous two sections, based on J, H, W1 and W2 magnitudes and by adopting the spectral type T5.5. We obtain $d = 20.0 \pm 2.0$ pc. The excellent agreement between the independent distance estimates for the two objects supports a binary classification. In the following we adopt the weighted average $d = 20.7 \pm 1.4$ pc as the distance to 2M1348-1344 binary. At this distance, the projected separation of $67.6'' \pm 0.3''$ is equivalent to 1400 ± 90 AU.

Following the same procedure as in Section 4.2, we obtain $T_{\text{eff}} \approx 2960 \pm 20$ K, and $\log(L/L_{\odot}) = -2.42 \pm 0.03$ for the primary. The activity lifetime for M4 dwarfs is 4.5 ± 0.5 Gyr. From the lack of $\text{H}\alpha$ emission in the spectrum of 2M1348-1344A, we place a lower limit for its age at 4 Gyr. The ζ -index of 2M1348-1344A is found to be very close to unity ($\zeta_{LRS} = 1.08$, $\zeta_D = 1.06$), placing the object into the dwarf metallicity class. The photometric relation of Schlaufman & Laughlin (2010) results in $[\text{Fe}/\text{H}] = -0.33 \pm 0.08$. Here we have to take into account the rms dispersion of the relation that equals 0.19 ± 0.03 , as calculated by Neves et al. (2012). Our result for the metallicity of 2M1348-1344A is therefore in agreement with the values found for other M-dwarfs in the solar neighbourhood, which have the mean $[\text{Fe}/\text{H}] = -0.17 \pm 0.07$ (Schlaufman & Laughlin 2010). The estimate for the mass of the primary gives $0.18 \pm 0.01 M_{\odot}$ (BCAH98, age 5-10 Gyr). The same number is obtained by following the relationship of Delfosse et al. (2000). For the T5.5 secondary, we obtain $T_{\text{eff}} \approx 1070 \pm 130$ K, and $\log(L/L_{\odot}) = -5.03 \pm 0.21$. Using COND03 (Baraffe

¹² Photographic R_F magnitude from GSC-II equivalent to the Johnson-Cousins R_C (Reid et al. 1991; Kirk et al. 2009).

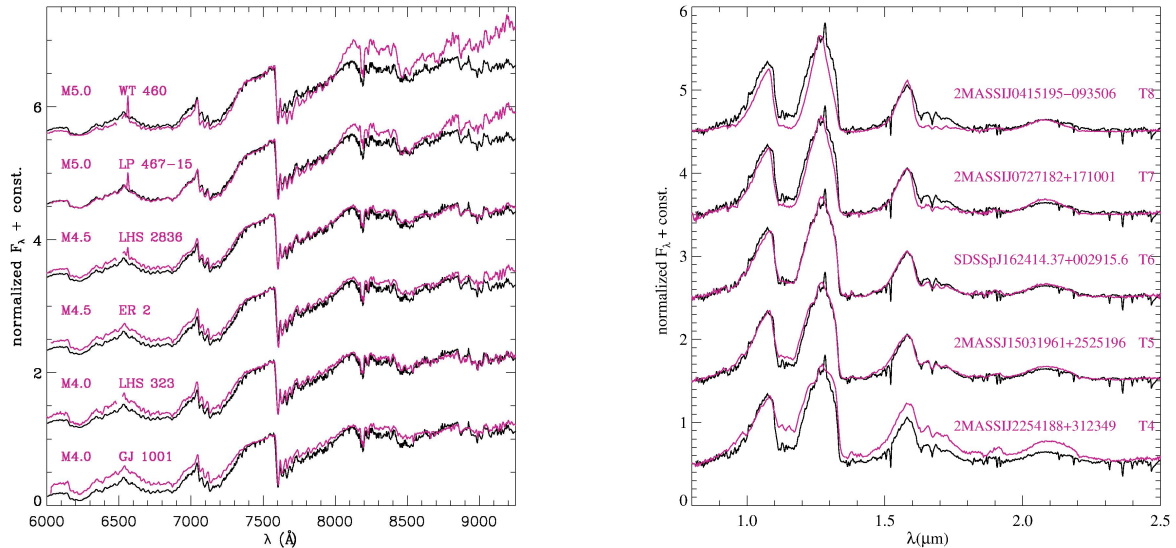


FIG. 6.— **Left:** EFOC2 spectrum of 2M1348-1344A shown in black, with the M-dwarf spectral sequence from dwarfarchives.org overplotted in purple. The comparison spectra were chosen to have broad wavelength coverage similar to our data, and were smoothed to match the resolution of the object spectrum. All spectra were normalized at 7500 Å. **Right:** FIRE spectrum of 2M1348-1344B shown in black, with the standard spectral sequence of T dwarfs (Burgasser et al. 2004, 2006a). The higher-resolution FIRE spectrum was smoothed to match the resolution of the spectral standards. All spectra were normalized at 1.25 μm.

et al. 2003) evolutionary models, we find the mass of the secondary to be $0.04 \pm 0.01 M_{\odot}$ for ages 5-10 Gyr. As in the case of 2M0525-7425, we find a relatively low mass ratio of 0.22 ± 0.06 . A summary of the observational and physical properties of 2M1348-1344 is given in Table 2.

2M1348-1344B is one of only a handful of known late T ($\geq T5$) wide companions to low mass stars, and one of only six late T dwarfs separated by more than 1000 AU from their primary stars. The other objects include Gl 570D (K4/M1.5/M3/T7 system, K4 and T7 separated by 3600 AU; Burgasser et al. 2000), ϵ Indi Bb (K5/T1/T6 system, K5 separated by 1460 AU from the T1-T6 close binary; Scholz et al. 2003; McCaughrean et al. 2004), Ross 458C (M0/M7/T8.5, M0 and T8.5 separated 1170 AU; Scholz 2010; Goldman et al. 2010; Burgasser et al. 2010b; Burningham et al. 2011), Hip 73786B (K5/T6p with separation of 1200 AU; Scholz 2010; Murray et al. 2011), and G204-39B (M3/T6.5 separated by 2685 AU; Faherty et al. 2010).

5. DISCUSSION

5.1. Stability of the wide binaries

Figure 7 shows the total mass versus separation for a sample of binary systems. We show the suggested empirical limits for the stability of VLM multiples from the studies of Reid et al. (2001) and Burgasser et al. (2003), based on objects that were known at the time of the respective works. Neither cutoff seems appropriate for the collection of widely separated systems plotted (see discussions in Faherty et al. 2010 and Dhital et al. 2010). The log-normal limitation on the separation of binaries found by Dhital et al. (2010) does encompass 2M0525-7425AB and all low-mass objects in Figure 7. Zuckerman & Song (2009) derived a cutoff for the binding energy of a system formed by fragmentation as a function of the total system mass, assuming separations of 300 AU. Since a number of systems found in the field and young clusters are found at separations larger than 300 AU, Faherty

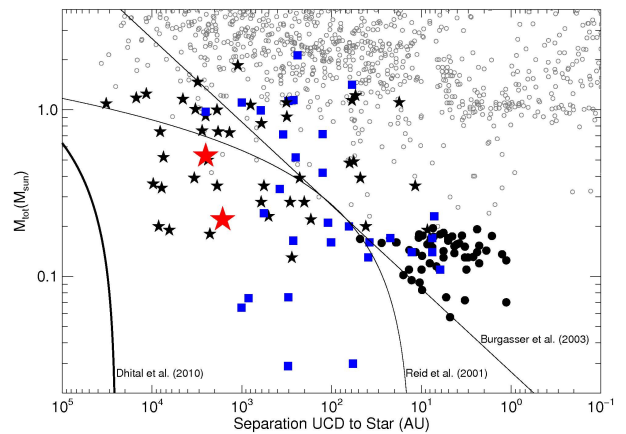


FIG. 7.— A plot of the total mass vs. binary separation. Objects marked with filled circles are tight low-mass systems. Wide systems (separation > 100 AU) containing a UCD companion are marked as five point stars and those marked as blue squares are systems containing a tight or widely separated UCD with an age < 500 Myr. Objects marked by open circles come from stellar companion catalogs. The new wide systems reported in this work are marked as red five-point stars. We have over-plotted the Reid et al. (2001) curve (center) which distinguished the cut-off for the formation of wide stellar pairs as well as the Burgasser et al. (2003) line (specific for $M_{tot} < 0.2 M_{\odot}$ field systems) and the log-normal limitation for systems with $M_{tot} > 0.3 M_{\odot}$ found in Dhital et al. (2010). Data were taken from Figure 9 in Faherty et al. (2011), see references therein for more details.

et al. (2010) used the Jeans length instead of the fiducial value of 300 AU to repeat the calculation for two extreme mass ratio cases. Both 2M0525-7425AB and 2M1348-1344 are found above the Zuckerman & Song (2009) and Faherty et al. (2010) limits.

Dhital et al. (2010) calculate the average binary lifetimes, that generally depend on the total mass and separation (see their Figure 19). With the parameters calculated in the previous sections, both systems reported here appear to be stable enough to survive longer than

TABLE 2
PHYSICAL PROPERTIES OF 2M1348-1344AB, 2M0525-7425AB, AND 2M0614+3950

	2M1348-1344A	2M1348-1344B	2M0525-7425A	2M0525-7425B	2M0614+3950
2MASS designation	13480721-1344321	13480290-1344071	05254550-7425263	05253876-7426008	06143818+3950357
$\mu_{\alpha} \cos \delta$ (mas yr ⁻¹)	-680 ± 28	-657 ± 23	270 ± 18	279 ± 18	-46 ± 21
μ_{δ} (mas yr ⁻¹)	-511 ± 32	-535 ± 33	308 ± 23	310 ± 23	-265 ± 23
Spectral type	M4.5 ± 0.5 ^b	T5.5 ± 1 ^c	M3.0 ± 0.5 ^b	L2 ^{a,b}	L9 ± 1 ^c
Distance (pc)	21.5 ± 2.1	20.0 ± 2.0	43.9 ± 4.3	48.0 ± 4.3	26.0 ± 1.8
T_{eff} (K)	2960 ± 20	1070 ± 130	3320 ± 50	1970 ± 120	1350 ± 110
Mass (M_{\odot})	0.18 ± 0.02	0.04 ± 0.01	0.46 ± 0.01	0.070 ^{+0.005} _{-0.010}	0.04 – 0.07
Age (Gyr)	≥ 4.0		≥ 1.5		
[Fe/H] ^d	-0.33 ± 0.08		-0.01 ± 0.03		
Angular separation (")		67.6 ± 0.3		43.9 ± 0.1	
Projected separation (AU)		1400 ± 90		2020 ± 130	
Binding energy (10 ⁴¹ erg)		0.91 ± 0.26		2.81 ± 0.45	
Mass ratio		0.22 ± 0.06		0.15 ± 0.02	

^a Kirkpatrick et al. (2010)

^b optical spectral type

^c NIR spectral type

^d Photometric relation from Schlaufman & Laughlin (2010)

10 Gyrs. Based on the component proper motions, excellent agreement in the independent distance estimates of each component, and stability arguments, we conclude that 2M0525-7425AB and 2M1348-1344AB are genuine binary systems.

5.2. Mass-ratios

Both wide binary systems reported in this work have relatively low mass ratios ($q = 0.22$ for 2M1348-1344 and $q = 0.15$ for 2M0525-7425). By analyzing a catalog of 1342 very-wide (projected separations of $\gtrsim 500$ AU) low-mass (at least one mid-K to mid-M dwarf component) binaries, Dhital et al. (2010) find the distribution of mass ratios to be strongly skewed toward equal-mass pairs: 85.5% of pairs have masses within 50% of each other. The authors conclude that this does not result from observational biases, i.e. the survey is sensitive to pairs with much lower mass ratios. A similar result is obtained by (Reid & Gizis 1997) in the volume-complete 8-pc sample, constituted mostly (80%) of M-dwarfs. However, the sensitivity to mass ratios in both works is reported for the entire samples, rather than for M dwarfs alone, and the sensitivity to low mass ratio systems will fall off with lower-mass primaries. In a study of multiplicity among M-dwarfs, Fischer & Marcy (1992) found that the distribution of mass ratios is flat and perhaps declines at low mass ratios. A number of low- q binary systems containing ultracool components are known to date, some with the mass-ratios as low as 0.05 (e.g. Faherty et al. 2010 and references therein). A complete sample sensitive to ultracool dwarfs of the very lowest masses is needed to assess the distribution of mass ratios in this regime.

5.3. Higher-order multiplicity

It has been found that binaries wider than ~ 100 AU have a high rate of tertiaries, both in the stellar and substellar regimes, and that the binary fraction of ultracool companions found in multiple systems appears to be significantly larger than that of field dwarfs (Burgasser et al. 2005; Tokovinin et al. 2006; Law et al. 2010; Faherty et al. 2010). This behavior has also been predicted by some dynamical models (Sterzik & Durisen 2003; Delgado-Donate et al. 2004; Whitworth & Sta-

matellos 2006; Kouwenhoven et al. 2010). Furthermore, dwarfs with spectral types of late L or early T show a higher multiplicity fraction compared to other types (Liu et al. 2006; Burgasser et al. 2006b; but see also Goldman et al. 2008). This has been attributed to the rapid evolution through the L/T transition phase, implying fewer sources per spectral subtype for a given field sample (Burgasser 2007). Unresolved binaries can be identified by an apparent over-luminosity for a given spectral subtype, where an independent distance estimate is available (e.g. Dupuy & Liu 2012), or by spectral deviations from template spectra (e.g. Burgasser et al. 2010a). Burgasser et al. (2010a) identified several common trends that stand out when comparing the combined near-infrared spectra of resolved L/T binaries with the template spectra of single objects.

The SpeX spectrum of the L/T transition dwarf 2M0614+3950 (Figure 2) is closely matched by the L9 spectral template, and does not show any of the deviations pointed out in Burgasser et al. (2010a). For the two wide binaries, 2M0525-7425AB and 2M1348-1344AB, the distance estimates of the primaries are in excellent agreement with the independent distance estimates of the secondaries. For example, by placing the T5.5 dwarf 2M1348-1344B at the distance of the primary augmented by its 1σ uncertainty +0.25 in its absolute J -magnitude, and -0.15 in its $J - H$ color, still consistent with the derived spectral type. Also, all of the component spectra presented here do not appear to deviate significantly from the spectral templates. We note that the classification of 2M0525-7425B originates from Kirkpatrick et al. (2010), who do not show a spectrum in the paper, but neither report any peculiarities. We conclude that, while we have no reason to suspect any unresolved binarity in the objects discussed here, high resolution imaging and/or radial velocity study is necessary to prove this claim.

5.4. Predictions from theory

Among the multiple systems produced in hydrodynamical simulations of star cluster formation by Bate (2009), about 10% are stars ($\geq 0.1 M_{\odot}$) with VLM ($< 0.1 M_{\odot}$) companions. About 30% of these star/VLM binary sys-

tems have semi-major axes larger than 1000 AU, and several objects with primary masses similar to those of the two systems reported here are created. Although there appears to be no statistically significant dependence of the frequency of star/VLM binaries on primary mass, the typical separation of such binaries seems to increase strongly with the primary mass. As for the mass ratios for the systems with $0.1 - 0.5 M_{\odot}$ primaries, Bate (2009) predicts a slight preference towards near-equal mass systems. However, a significant number of systems with low-mass ratios is produced in the simulations, with about 15% of the binaries having $q \leq 0.2$. Another prediction of this model is a correlation between mass ratio and separation for the binaries, with closer systems having a preference for equal masses. The median mass ratio for binary separations in range $1000 - 10^4$ AU is 0.17, comparable to the mass ratios observed in our two binary systems. Simulations by Stamatellos & Whitworth (2009) show that very wide (up to 10 000 AU), low-mass (secondary mass $< 80 M_J$) companions can be formed in fragmenting stellar disks. In the simulation of a $0.7 M_{\odot}$ star with a disk of an equal mass and a radius of 400 AU, wide (400-10 000 AU) binary companions to the central star are predominantly brown dwarfs. An alternative mechanism to form wide binaries was proposed by Kouwenhoven et al. (2010) and Moeckel & Clarke (2011). Their N-body simulations of star clusters in dissolution show that binaries with separations larger than 1000 AU can be formed by dynamical capture of initially unbound objects. While the wide binary fraction from Kouwenhoven et al. (2010) varies significantly with the initial conditions, by integrating over the initial cluster mass distribution they predict a wide binary fraction of a few percent in the Galactic field. For wide systems with separations > 1000 AU and primary masses below $1.5 M_{\odot}$, Kouwenhoven et al. (2010) models predict the increase in the number of the systems with decreasing the mass ratio. The mass-ratio distributions peaks around $q = 0.1 - 0.3$.

The existence of binaries with total system masses, mass ratios and separations similar to the two systems reported here is clearly supported by predictions of different theoretical models. A proper statistical analysis of complete wide binary samples is needed to assess their overall frequency and distribution of properties such as mass ratio, and to be able to compare these observational results with the predictions of the models.

6. SUMMARY AND CONCLUSIONS

We have presented the results of our search for common proper motion pairs containing ultracool components, based on 2MASS and Preliminary WISE data catalogs, followed by optical or NIR spectroscopy of individual candidate components. We report the discovery of two wide binaries containing ultracool components, and

one ultracool dwarf at the L/T transition.

2M1348-1344AB consists of a M4.5 primary with a T5.5 companion, at a distance ~ 20 pc from the Sun, and at separation of 1400 AU. An M3 primary and its L2 companion comprise the system 2M0525-7425AB, found lying at a distance ~ 45 pc, and separated by 2000 AU. Based on the matching proper motions and excellent agreement in distance estimates of the components, as well as on the fulfilled stability criteria, we conclude that both systems are genuine low-mass binaries. Both primaries are found to have metallicities close to that of our Sun, and lack H α emission, allowing us to place the lower limits on the ages of the two systems at 1.5 Gyr (2M0525-7425) and 4 Gyr (2M1348-1344). We also report the discovery of 2M0614+3950, an ultracool dwarf with spectral type L9, lying at a distance ~ 26 pc.

The three objects reported here add to the compendium of ultracool objects discovered by WISE, which is certain to grow with the recent survey's all sky release. Further characterization of the L/T transition dwarf and the components of the two new binary systems will provide stringent tests for understanding of ultracool atmospheres, as well as for the formation models of BDs and BD binaries. 2M1348-1344AB is particularly important in this sense, being one of a handful of known late-T very wide companions to low mass stars.

We thank David Lafrenière for his contribution to writing software used for this project. The research was supported in part by grants from the Natural Sciences and Engineering Research Council (NSERC) of Canada to R.J. R.J.'s work was also supported in part by the Radcliffe Institute for Advanced Study at Harvard University. R.K. acknowledges support from Cento de Astrofísica de Valparaíso and DIPUV 23/2009. S.M.'s work is supported by NASA through grant 10-ADAP10-0130. This work was co-funded under the Marie Curie Actions of the European Commission (FP7-COFUND). J.B. is supported by the Chilean Ministry for the Economy, Development, and Tourism's Programa Iniciativa Científica Milenio through grant P07-021-F, awarded to The Milky Way Millennium Nucleus and FONDECYT Reg. No. 1120601. This publication makes use of data products from the Two Micron All Sky Survey, which is a joint project of the University of Massachusetts and the Infrared Processing and Analysis Center/California Institute of Technology, funded by the National Aeronautics and Space Administration and the National Science Foundation. This research has benefited from the SpeX Prism Spectral Libraries, maintained by Adam Burgasser at <http://pono.ucsd.edu/~adam/browndwarfs/spexprism/>. This research has also benefited from the M-dwarf spectra available from <http://www.dwarffarchives.org>.

REFERENCES

- Ackerman, A. S. & Marley, M. S. 2001, *ApJ*, 556, 872
 Artigau, É., Bouchard, S., Doyon, R., & Lafrenière, D. 2009, *ApJ*, 701, 1534
 Bailer-Jones, C. A. L. & Mundt, R. 1999, *A&A*, 348, 800
 Baraffe, I., Chabrier, G., Allard, F., & Hauschildt, P. H. 1998, *A&A*, 337, 403
 —. 2002, *A&A*, 382, 563
 Baraffe, I., Chabrier, G., Barman, T. S., Allard, F., & Hauschildt, P. H. 2003, *A&A*, 402, 701
 Bate, M. R. 2009, *MNRAS*, 392, 590
 Bate, M. R. & Bonnell, I. A. 2005, *MNRAS*, 356, 1201
 Boffin, H. M. J., Watkins, S. J., Bhattal, A. S., Francis, N., & Whitworth, A. P. 1998, *MNRAS*, 300, 1189

- Bonfils, X., Delfosse, X., Udry, S., Santos, N. C., et al. 2005, *A&A*, 442, 635
- Burgasser, A. J. 2007, *ApJ*, 659, 655
- Burgasser, A. J., Cruz, K. L., Cushing, M., et al. 2010a, *ApJ*, 710, 1142
- Burgasser, A. J., Geballe, T. R., Leggett, S. K., Kirkpatrick, J. D., & Golimowski, D. A. 2006a, *ApJ*, 637, 1067
- Burgasser, A. J., Kirkpatrick, J. D., Cruz, K. L., et al. 2006b, *ApJS*, 166, 585
- Burgasser, A. J., Kirkpatrick, J. D., Cutri, R. M., et al. 2000, *ApJ*, 531, L57
- Burgasser, A. J., Kirkpatrick, J. D., & Lowrance, P. J. 2005, *AJ*, 129, 2849
- Burgasser, A. J., Kirkpatrick, J. D., Reid, I. N., et al. 2003, *ApJ*, 586, 512
- Burgasser, A. J., Marley, M. S., Ackerman, A. S., et al. 2002, *ApJ*, 571, L151
- Burgasser, A. J., McElwain, M. W., Kirkpatrick, J. D., Cruz, K. L., Tinney, C. G., & Reid, I. N. 2004, *AJ*, 127, 2856
- Burgasser, A. J., Simcoe, R. A., Bochanski, J. J., et al. 2010b, *ApJ*, 725, 1405
- Burningham, B., Leggett, S. K., Homeier, D., et al. 2011, *MNRAS*, 414, 3590
- Buzzoni, B., Delabre, B., Dekker, H., et al. 1984, *The Messenger*, 38, 9
- Casagrande, L., Flynn, C., & Bessell, M. 2008, *MNRAS*, 389, 585
- Chabrier, G., Baraffe, I., Allard, F., & Hauschildt, P. 2000, *ApJ*, 542, 464
- Cushing, M. C., Vacca, W. D., & Rayner, J. T. 2004, *PASP*, 116, 362
- Dahn, C. C., Harris, H. C., Vrba, F. J., et al. 2002, *AJ*, 124, 1170
- Deacon, N. R., Liu, M. C., Magnier, E. A., et al. 2012, *ApJ*, 757, 100
- Delfosse, X., Forveille, T., Ségransan, D., et al. 2000, *A&A*, 364, 217
- Delgado-Donate, E. J., Clarke, C. J., Bate, M. R., & Hodgkin, S. T. 2004, *MNRAS*, 351, 617
- Dhital, S., West, A. A., Stassun, K. G., & Bochanski, J. J. 2010, *AJ*, 139, 2566
- Dhital, S., West, A. A., Stassun, K. G., et al. 2012, *AJ*, 143, 67
- Dupuy, T. J. & Liu, M. C. 2012, *ApJS*, 201, 19
- Eisenhardt, P. R. M., Griffith, R. L., Stern, D., et al. 2010, *AJ*, 139, 2455
- Faherty, J. K., Burgasser, A. J., Bochanski, J. J., et al. 2011, *AJ*, 141, 71
- Faherty, J. K., Burgasser, A. J., Walter, F. M., et al. 2012, *ArXiv e-prints*
- Faherty, J. K., Burgasser, A. J., West, A. A., et al. 2010, *AJ*, 139, 176
- Fischer, D. A. & Marcy, G. W. 1992, *ApJ*, 396, 178
- Goldman, B. 2005, *Astronomische Nachrichten*, 326, 1059
- Goldman, B., Bouy, H., Zapatero Osorio, M. R., et al. 2008, *A&A*, 490, 763
- Goldman, B., Marsat, S., Henning, T., Clemens, C., & Greiner, J. 2010, *MNRAS*, 405, 1140
- Johnson, J. A. & Apps, K. 2009, *ApJ*, 699, 933
- Kirk, J. M., Ward-Thompson, D., Di Francesco, J., et al. 2009, *ApJS*, 185, 198
- Kirkpatrick, J. D., Cushing, M. C., Gelino, C. R., et al. 2011, *ApJS*, 197, 19
- Kirkpatrick, J. D., Looper, D. L., Burgasser, A. J., et al. 2010, *ApJS*, 190, 100
- Kirkpatrick, J. D., Reid, I. N., Liebert, J., et al. 2000, *AJ*, 120, 447
- Knapp, G. R., Leggett, S. K., Fan, X., et al. 2004, *AJ*, 127, 3553
- Kouwenhoven, M. B. N., Goodwin, S. P., Parker, R. J., et al. 2010, *MNRAS*, 404, 1835
- Kraus, A. L. & Hillenbrand, L. A. 2009, *ApJ*, 703, 1511
- Law, N. M., Dhital, S., Kraus, A., Stassun, K. G., & West, A. A. 2010, *ApJ*, 720, 1727
- Lépine, S. & Bongiorno, B. 2007, *AJ*, 133, 889
- Lépine, S., Hilton, E. J., Mann, A. W., et al. 2012, *ArXiv e-prints*
- Lépine, S., Rich, R. M., & Shara, M. M. 2007, *ApJ*, 669, 1235
- Liu, M. C., Leggett, S. K., Golimowski, D. A., et al. 2006, *ApJ*, 647, 1393
- Longhitano, M. & Binggeli, B. 2010, *A&A*, 509, A46
- Looper, D. L., Kirkpatrick, J. D., & Burgasser, A. J. 2007, *AJ*, 134, 1162
- Loutrel, N. P., Luhman, K. L., Lowrance, P. J., & Bochanski, J. J. 2011, *ApJ*, 739, 81
- Low, C. & Lynden-Bell, D. 1976, *MNRAS*, 176, 367
- McCaughrean, M. J., Close, L. M., Scholz, R.-D., et al. 2004, *A&A*, 413, 1029
- Moeckel, N. & Clarke, C. J. 2011, *MNRAS*, 415, 1179
- Murray, D. N., Burningham, B., Jones, H. R. A., et al. 2011, *MNRAS*, 414, 575
- Neves, V., Bonfils, X., Santos, N. C., et al. 2012, *A&A*, 538, A25
- Padoan, P. & Nordlund, Å. 2004, *ApJ*, 617, 559
- Pinfield, D. J., Jones, H. R. A., Lucas, P. W., et al. 2006, *MNRAS*, 368, 1281
- Radigan, J., Jayawardhana, R., Lafrenière, D., et al. 2012, *ArXiv e-prints*
- Radigan, J., Lafrenière, D., Jayawardhana, R., & Doyon, R. 2008, *ApJ*, 689, 471
- , 2009, *ApJ*, 698, 405
- Rayner, J. T., Toomey, D. W., Onaka, P. M., et al. 2003, *PASP*, 115, 362
- Reid, I. N., Brewer, C., Brucato, R. J., et al. 1991, *PASP*, 103, 661
- Reid, I. N. & Cruz, K. L. 2002, *AJ*, 123, 2806
- Reid, I. N., Cruz, K. L., Allen, P., et al. 2003, *AJ*, 126, 3007
- Reid, I. N. & Gizis, J. E. 1997, *AJ*, 113, 2246
- Reid, I. N., Gizis, J. E., Kirkpatrick, J. D., & Koerner, D. W. 2001, *AJ*, 121, 489
- Reipurth, B. & Clarke, C. 2001, *AJ*, 122, 432
- Schlaufman, K. C. & Laughlin, G. 2010, *A&A*, 519, A105
- Scholz, R.-D. 2010, *A&A*, 515, A92
- Scholz, R.-D., McCaughrean, M. J., Lodieu, N., & Kuhlbrodt, B. 2003, *A&A*, 398, L29
- Simcoe, R. A., Burgasser, A. J., Bernstein, R. A., et al. 2008, in *Society of Photo-Optical Instrumentation Engineers (SPIE) Conference Series*, Vol. 7014
- Simcoe, R. A., Burgasser, A. J., Bochanski, J. J., et al. 2010, in *Society of Photo-Optical Instrumentation Engineers (SPIE) Conference Series*, Vol. 7735
- Stamatellos, D. & Whitworth, A. P. 2009, *MNRAS*, 392, 413
- Stephens, D. C., Leggett, S. K., Cushing, M. C., et al. 2009, *ApJ*, 702, 154
- Sterzik, M. F. & Durisen, R. H. 2003, *A&A*, 400, 1031
- Subasavage, J. P., Henry, T. J., Hambly, N. C., Brown, M. A., & Jao, W.-C. 2005, *AJ*, 129, 413
- Tinney, C. G., Burgasser, A. J., & Kirkpatrick, J. D. 2003, *AJ*, 126, 975
- Tinney, C. G. & Tolley, A. J. 1999, *MNRAS*, 304, 119
- Tokovinin, A., Thomas, S., Sterzik, M., & Udry, S. 2006, *A&A*, 450, 681
- Vacca, W. D., Cushing, M. C., & Rayner, J. T. 2003, *PASP*, 115, 389
- West, A. A., Hawley, S. L., Bochanski, J. J., et al. 2008, *AJ*, 135, 785
- Whitworth, A. P. & Stamatellos, D. 2006, *A&A*, 458, 817
- Whitworth, A. P. & Zinnecker, H. 2004, *A&A*, 427, 299
- Zacharias, N., Monet, D. G., Levine, S. E., et al. 2005, *VizieR Online Data Catalog*, 1297, 0
- Zuckerman, B. & Song, I. 2009, *A&A*, 493, 1149